A NEW METHOD FOR ANALYZING ^{14}C OF METHANE IN ANCIENT AIR EXTRACTED FROM GLACIAL ICE

Vasilii V Petrenko[1,2] • Andrew M Smith[3] • Gordon Brailsford[4] • Katja Riedel[4] • Quan Hua[3] • Dave Lowe[4] • Jeffrey P Severinghaus[1] • Vladimir Levchenko[3] • Tony Bromley[4] • Rowena Moss[4] • Jens Mühle[1] • Edward J Brook[5]

ABSTRACT. We present a new method developed for measuring radiocarbon of methane ($^{14}CH_4$) in ancient air samples extracted from glacial ice and dating 11,000–15,000 calendar years before present. The small size (~20 µg CH_4 carbon), low CH_4 concentrations ([CH_4], 400–800 parts per billion [ppb]), high carbon monoxide concentrations ([CO]), and low ^{14}C activity of the samples created unusually high risks of contamination by extraneous carbon. Up to 2500 ppb CO in the air samples was quantitatively removed using the Sofnocat reagent. ^{14}C procedural blanks were greatly reduced through the construction of a new CH_4 conversion line utilizing platinized quartz wool for CH_4 combustion and the use of an ultra-high-purity iron catalyst for graphitization. The amount and ^{14}C activity of extraneous carbon added in the new CH_4 conversion line were determined to be 0.23 ± 0.16 µg and 23.57 ± 16.22 pMC, respectively. The amount of modern (100 pMC) carbon added during the graphitization step has been reduced to 0.03 µg. The overall procedural blank for all stages of sample handling was 0.75 ± 0.38 pMC for ~20-µg, ^{14}C-free air samples with [CH_4] of 500 ppb. Duration of the graphitization reactions for small (<25 µg C) samples was greatly reduced and reaction yields improved through more efficient water vapor trapping and the use of a new iron catalyst with higher surface area. ^{14}C corrections for each step of sample handling have been determined. The resulting overall $^{14}CH_4$ uncertainties for the ancient air samples are ~1.0 pMC.

INTRODUCTION

CH_4 is the most abundant organic molecule in the Earth's atmosphere and a key player in global atmospheric chemistry (Brasseur et al. 1999). It is also the third most important greenhouse gas after H_2O and CO_2, with a global warming potential 25 times that of CO_2 on a 100-yr timescale (Forster et al. 2007). Ice-core records from Greenland and Antarctica show large and rapid variations in atmospheric CH_4 concentrations ([CH_4]) in response to climate change (Chappellaz et al. 1993; Brook et al. 2000). Ice-core records and measurements from firn air, as well as direct instrumental measurements of the atmosphere, also capture the rapid rise of [CH_4] starting around AD 1750, which is attributed to anthropogenic activity (Etheridge et al. 1998).

Measurements of atmospheric $^{14}CH_4$ in the past 2 decades have helped to constrain the fossil CH_4 contribution to the global budget, as well as reveal the $^{14}CH_4$ rise due to production from pressurized-water reactors (PWRs), though much uncertainty in these source terms remains (Conny and Currie 1996; Lassey et al. 2007). ^{14}C can be a similarly powerful tool for understanding paleo-CH_4 budgets and changes in the CH_4 sources during rapid climatic transitions at the end of the last glacial period. Recent studies of δD and $\delta^{13}C$ of CH_4 have been able to put constraints on CH_4 budgets during the last glacial termination (Schaefer et al. 2006; Sowers 2006). However, the uncertainties and similarities in the δD and $\delta^{13}C$ signatures of many paleo-CH_4 sources stand in the way of definitive CH_4 budget reconstructions. Here, $^{14}CH_4$ has the great advantage of being able to definitively separate the biogenic sources (wetlands, plants, animals) from geologic and clathrate sources. Biogenic $^{14}CH_4$ mostly follows atmospheric $^{14}CO_2$ (Wahlen et al. 1989; Quay et al. 1999), while most geo-

[1]Scripps Institution of Oceanography, University of California, San Diego, Mail Code 0244, 9500 Gilman Dr., La Jolla, California 92093, USA.
[2]Corresponding author. Email: vpetrenko@ucsd.edu.
[3]Australian Nuclear Science and Technology Organisation (ANSTO), PMB 1, Menai, NSW 2234, Australia.
[4]National Institute of Water and Atmospheric Research, Private Bag 14901, Wellington, New Zealand.
[5]Department of Geosciences, Oregon State University, Corvallis, Oregon 97331, USA.

logic and clathrate sources are very old and either contain no measurable ^{14}C or very low ^{14}C levels (Winckler et al. 2002; Grabowski et al. 2004; Kessler et al. 2006).

It has been suggested that several large and rapid atmospheric CH_4 increases during the last 100 kyr were the result of massive climate-driven destabilization of marine methane clathrates, which then in turn contributed to the warming (Kennett et al. 2000, 2003). Quantifying clathrate contributions to the CH_4 increases during abrupt warming events at the end of the last glacial period is particularly relevant in the light of current anthropogenic warming. By recent estimates, the present amount of CH_4 carbon associated with clathrates is 500–5000 Pg (Buffett and Archer 2004; Milkov 2004), which at the upper end is comparable to the estimated carbon content of all the fossil fuels. Future warming of the oceans may destabilize large amounts of methane clathrate, providing a substantial positive feedback to the warming.

At present, methods already exist for [14]CH_4 analyses on modern atmospheric air, as well as on ocean water (Lowe et al. 1991; Kessler and Reeburgh 2005). Here, we describe the techniques developed to perform the first [14]CH_4 measurements on ancient air extracted from glacial ice. Ice cores are commonly used for paleo-atmospheric studies, but at least 1000 kg of ancient ice is required to provide ~25 micrograms of CH_4-derived carbon (µg C), barely enough for measurement of ^{14}C by accelerator mass spectrometry (AMS). Such large amounts of ancient ice of a uniform age are not available from deep ice cores.

Previous work has shown that large amounts of ancient ice dating to the last glacial termination outcrop at the Pakitsoq ablation site in West Greenland, presenting a "horizontal ice core" at the surface (Reeh et al. 1991; Petrenko et al. 2006). The CH_4 record in Pakitsoq ice was shown to be mostly well preserved. However, elevated CH_4 values (with respect to the GISP2 ice-core record) were found in some ice sections (Petrenko et al. 2006). Ancient air samples (~100 L each) for [14]CH_4 analyses with ages between 11–15 calendar kyr BP were obtained from Pakitsoq ice by melt-extraction in the field (hereafter referred to as "Pakitsoq samples") and details are presented in Petrenko et al. (2008). Briefly, ice containing ancient air of the required age was cut with oil-free electric chainsaws from 0.5–2.5 m below the surface. The air extraction was carried out immediately by melting the ice under vacuum in a ~670-L chemically polished and anodized aluminum chamber. The released air was then transferred to 35-L electropolished stainless steel cylinders using oil-free diaphragm pumps. The air was stored in these cylinders until being processed for [14]CH_4. Accurate determination of gas ages in the sampled ice was achieved (uncertainties in absolute mean gas age for all large air samples were <300 yr) by comparing records of $\delta^{15}N$ of N_2, $\delta^{18}O$ of O_2, [CH_4], and $\delta^{18}O_{ice}$ in near-surface horizontal sample profiles at Pakitsoq with the GISP2 ice-core record of these tracers (Petrenko et al. 2006, 2008).

The [CH_4] blank for the melt-extractions was found to be <4 ppb for all samples. Repeated measurements of [CH_4] in the Pakitsoq air samples over the storage period (1–2 yr) showed that [CH_4] was stable for all samples. Measurements of $\delta^{18}O$ of O_2 and $\delta^{15}N$ of N_2 in the samples indicated no significant gas isotopic fractionation from the melt-extraction. Ar/N_2, CFC-11, and CFC-12 measured in the samples indicated no significant [14]CH_4 contamination from ambient air. Ar/N_2, Kr/Ar, and Xe/Ar ratios in the samples were used to quantify effects of gas dissolution during the melt-extractions and correct the sample [CH_4]. [CH_4] values corrected for blank and solubility effects were slightly elevated over expected values for most samples. This may be due to a small amount of microbial in situ CH_4 production in the ice (Price 2007). Two of the samples had [CH_4] substantially elevated with respect to contemporaneous GISP2 ice (by >60 ppb). [14]CH_4 measured in these 2 samples allows for small [14]CH_4 corrections to be made for other samples for this inferred in situ-produced CH_4 component.

^{14}CH$_4$ in all the samples has been successfully analyzed and the results will be presented elsewhere. In this paper, we present the techniques developed for CH$_4$ extraction from air and combustion to CO$_2$ as well as for graphitization and measurement of these samples by AMS. Exceptionally low levels of extraneous ^{14}C from processing are essential for minimizing the uncertainties of results with such small, ^{14}C-depleted samples. We discuss how this has been achieved, as well as the methods for accurately determining procedural ^{14}C corrections for each part of the sample handling.

EXTRACTION OF CH$_4$ FROM THE AIR STREAM AND COMBUSTION TO CO$_2$

Description of the CH$_4$ Conversion Line

A new CH$_4$ conversion line was developed at the National Institute of Water and Atmospheric Research (NIWA) in Wellington, New Zealand, for processing the Pakitsoq samples (Figure 1) after methods described by Lowe et al. (1991), but utilizing different CH$_4$ combustion and CO oxidation catalysts. Air entering this line passes first through a thimble trap and then a "Russian doll" trap with nested glass fiber thimbles (Brenninkmeijer 1991) (both at liquid nitrogen (LN$_2$) temperature) to remove H$_2$O, CO$_2$, N$_2$O, and non-methane volatile organic compounds (VOCs). The air stream is then stripped of CO through oxidation to CO$_2$ on Sofnocat 423 (Molecular Products Group LTD, Essex, United Kingdom) at room temperature followed by cryogenic removal of this CO$_2$ using 2 further Russian doll traps at LN$_2$ temperature. The air stream then passes through a furnace consisting of ~1 g of platinized quartz wool (Shimadzu Scientific Instruments, USA) packed to a length of ~55 mm into a 25-mm-ID quartz tube at ~700 °C, where CH$_4$ is combusted to CO$_2$. The resulting CO$_2$ is captured in 3 LN$_2$-cooled traps. Air is pulled through the line by a 2-stage rotary vane pump.

The use of platinized quartz wool allowed the elimination of sample ^{14}C "memory" effects that were determined to be significant with platinized alumina pellets (data not shown), previously used for CH$_4$ combustion. This is most likely due to the fact that quartz wool has lower surface area and is a less porous substrate than alumina pellets, as well as that a much smaller amount of the catalyst was used (~1 g in the new CH$_4$ line vs. ~200 g in the pre-existing line). Further, a pre-existing CH$_4$ conversion line (utilizing platinized alumina) was shown to have a ^{14}CH$_4$ blank of ~3 pMC for 20–30 µg C test samples containing ~500–600 ppb of fossil CH$_4$ in ultra-high-purity (uhp) air, which was unacceptable for the Pakitsoq samples. The new line dramatically reduced the ^{14}C blank (see section "Corrections for CH$_4$ Extraction Line Blank" and Table 4) by utilizing a small amount of platinized quartz wool catalyst, as well as having a small internal volume (<700 cm^3 total) and surface area.

CH$_4$ Conversion Line Procedure

To minimize the carbon blank and sample memory, the line was kept evacuated while not in use. Quantitative leak checks were performed on both the upstream and downstream parts of the line at the start of each day to ensure that any extraneous carbon added from leaks during a sample run would not exceed 0.1% of the total sample carbon. Leak checks were also performed on all connections to tanks containing sample, blank, and reference gases. The furnace temperature was kept constant at 697–698 °C. Prior to starting a sample run, the line was flushed with CH$_4$-free uhp air at 0.8 standard liters (SL)/min for 15 min. A 1-hr-long flush followed any high [CH$_4$] (~28 ppm) blank samples or larger than usual (>25 µg C) samples of modern air (see Table 4), to make certain the line was purged of residual carbon from these samples.

The flow of sample air (also at 0.8 SL/min) was started immediately after stopping the flow of the flush gas. CO$_2$ collection downstream of the furnace was started 3 min after starting the flow of the sample air. The LN$_2$ in all traps was topped up every 10 min and the glass stem valves downstream
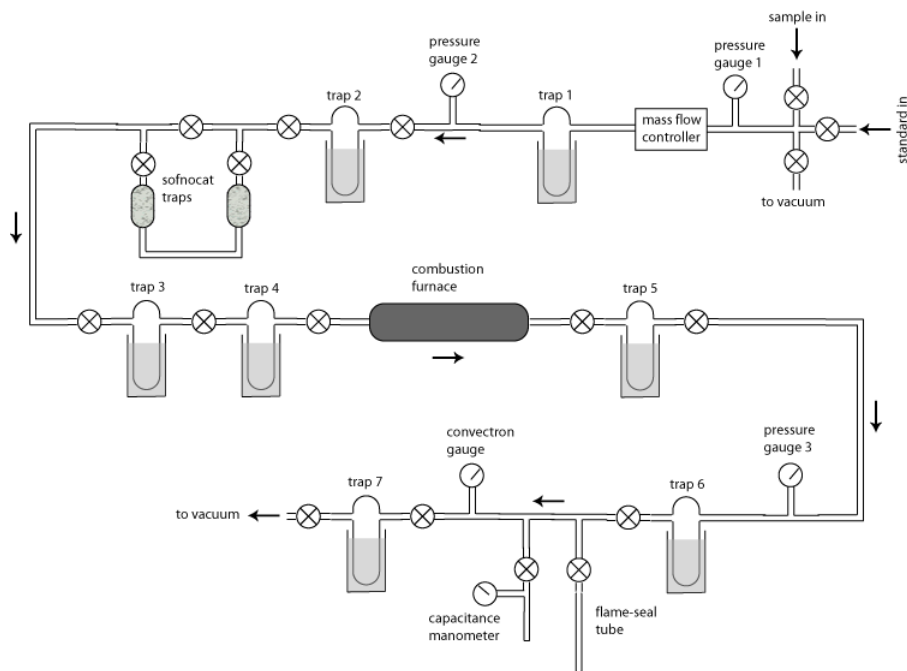
Figure 1 A schematic illustration of the new CH_4 extraction line developed for processing ancient Pakitsoq air samples for $^{14}CH_4$. The inlet allows for evacuation of the stainless steel flex hose that connects to the sample tank, minimizing the amount of gas wasted during the line flush. A 30-bar gauge is used to monitor the inlet pressure, and the air flow is kept at 0.8 SL/min with a Teledyne-Hastings mass flow controller (MFC). All the traps are cooled with liquid nitrogen. Trap 1 is a stainless steel thimble trap. Traps 2–4 are "Russian doll"-type traps (Brenninkmeijer 1991). Traps 5 and 7 are Pyrex® U-traps, and trap 6 is a 6-mm-OD Pyrex multiloop trap. Gauges 2 and 3 are Pirani-type gauges. The Sofnocat 423 reagent is in 2 glass bulbs covered with aluminum foil to protect from direct light. The combustion furnace is a 25-mm-ID quartz tube packed with platinum-coated quartz wool catalyst.

of the traps were warmed with a heat gun every 10 min (earlier tests determined that there was a risk of small leaks through the valves if they became too cold). Typical line pressures at gauges 2 and 3 (Figure 1) during a run were 260 and 55 mbar, respectively. After completing the sample collection, the resulting CO_2 was vacuum-distilled using LN_2 and an ethanol/dry ice mixture to separate it from the H_2O (produced during CH_4 combustion). The sample size was determined in a small calibrated volume using a capacitance manometer, and the sample CO_2 was then flame-sealed in a precleaned 6-mm Pyrex® tube. Prior to starting the next sample, the furnace was evacuated to <0.05 mbar, and the entire line to <1 mbar. If the previous sample contained a lot of moisture (such as all the Pakitsoq samples and melt-extraction blanks), all the upstream traps were also dried prior to starting the next sample.

The Pakitsoq air samples were saturated with H_2O vapor because the samples were not dried during the melt-extraction. Tests suggested that the upstream LN_2-cooled traps could become blocked with ice in the duration of a sample run. To lower the H_2O vapor pressure in the sample tanks and reduce the risk of ice buildup in traps, sample tanks were kept in a bucket of ice while being processed. However, this introduced the possibility of a slight thermal fractionation of the CH_4 isotopes between the top and the bottom of the tank. In addition, to utilize the maximum amount of sample possible, the sample tanks were run down to a pressure of 0.3 bar (initial pressures in all Pakitsoq

sample tanks were 2–3 bar). It was suspected that some isotopic fractionation could also be caused by the mass flow controller at these low tank pressures. A test was conducted to check the possible effects on sample yield and $\delta^{13}C$ of cooling the sample tank and running it down to 0.3 bar. No significant differences relative to control runs were found in either yield or $\delta^{13}C$ (Test 4 in Table 2).

High [CO] and ^{14}C of CO in Pakitsoq Ancient Air Samples

A further complication in processing air samples extracted from glacial ice for $^{14}CH_4$ is the possibility of ^{14}C contamination from CO. Any CO in the samples that breaks through the CO-oxidizing reagent in the line is oxidized to CO_2 in the furnace, and this CO_2 is then collected along with CH_4-derived CO_2. Air samples extracted from Pakitsoq ice contain very high [CO] (800–2500 ppb) as compared to modern ambient air concentrations (40–200 ppb). The fact that this high [CO] is not an artifact of the melt-extraction is confirmed by the low [CO] in the extraction blanks (20–40 ppb), as well as by independent measurements of [CO] in Pakitsoq ice conducted at Washington State University, which yielded values in excess of 800 ppb (unpublished). The source of this extremely high [CO] is not well understood. Haan and Raynaud (1998) measured [CO] in Greenland ice-core samples, and for gas ages between AD 1000 and 1600 found concentrations between 100 and 180 ppb, high variability, and a general trend of [CO] increasing with age. They suggest the slow oxidation of organic matter in Greenland ice as the most likely explanation. Colussi and Hoffmann (2003) suggest that the same data can be explained by photolysis of organic matter by UV Cerenkov radiation from cosmic muons passing through the ice. It is thus likely that our very high [CO] originates from organic matter in the ice.

CO is of concern because carbon-14 of CO (^{14}CO) in glacial ice can be elevated, owing to in situ cosmogenic production in the upper ~10 m of the firn (Lal et al. 2000). Energetic ^{14}C is produced by neutron-induced spallation of oxygen nuclei in the ice crystals, and most of it is quickly oxidized to either ^{14}CO or $^{14}CO_2$. Some of the resulting ^{14}CO remains trapped in the ice crystal lattice; however, it may also be expelled into the interstitial spaces and lost back to the atmosphere during recrystallization of the firn. A study by Lal et al. (2000) on 12 GISP2 ice samples between 125 and 1838 m depth found ^{14}CO concentrations ranging between 10 and 930 ^{14}CO molecules g^{-1} of ice, with an average of 298 molecules g^{-1} ice; although other studies of ^{14}CO and $^{14}CO_2$ in deep ice cores have found much lower values (Smith et al. 2000; Van de Wal et al. 2007). Two early measurements of ^{14}CO in Pakitsoq samples, done by dilution, yielded 38 ^{14}CO molecules g^{-1} ice, with the possible range of values being 0–83 molecules g^{-1} ice (the large uncertainty arises from the dilution factor of ~1:600). For comparison, ice containing air of Younger Dryas age (~12,000 calendar yr BP) is expected to contain only about 0.5 $^{14}CH_4$ molecules g^{-1} ice (in air bubbles). Thus, quantitative removal of CO was essential to ensure that ^{14}CO did not interfere with sample $^{14}CH_4$.

To address this problem, 2 Sofnocat 423 traps in series, each containing ~10 g of the reagent, were used to oxidize CO to CO_2, followed by cryogenic removal with 2 LN_2-cooled Russian doll traps in series (Figure 1). Sofnocat has been previously shown to be very effective at CO oxidation (Foulger and Simmonds 1993). Table 1a summarizes our preliminary tests with Sofnocat 423 and Table 1b shows the results of CO removal tests with Sofnocat conducted on the new CH_4 conversion line immediately prior to processing the Pakitsoq air samples for $^{14}CH_4$. As can be seen, even small amounts of Sofnocat can quantitatively remove up to 7000 ppb of CO. The [CH_4] values in the test gas prior to and after passing through the Sofnocat indicate that CH_4 is unaffected. Tests conducted on the new CH_4 line indicate that the CO removal factor is at least 500× for each part of the Sofnocat trap (comparing test results with the [CO] blank and taking [CO] measurement errors into consideration). The minimal CO removal factor for the 2 parts of the Sofnocat trap combined in series is then 250,000. At this removal efficiency and assuming a maximum ^{14}CO of 83 molecules per gram of ice

for Pakitsoq samples (upper range of measurements listed above), the ^{14}C from CO that breaks through the Sofnocat would amount to <0.1% of the expected ^{14}C from CH_4 and is thus negligible.

Table 1a Summary of tests conducted with the Sofnocat 423 reagent. For tests shown in (a), a gas mixture containing ~500 ppb CH_4 and high CO was passed first through the Sofnocat 423 reagent, then through a mass flow controller. Sofnocat (12.11 g) was packed into a 13-mm-OD stainless steel tube to a length of 8 ± 0.5 cm. Gas aliquots were taken for gas chromatography (GC) measurements just upstream and just downstream of the Sofnocat. Pressure was maintained at 2 bar. The 3.4 ppb of CO remaining in the first test is most likely due to residual CO in the gas chromatograph from an immediately prior measurement of standard gas. The small variations in $[CH_4]$ measured upstream and downstream of the Sofnocat are not significant. Tests shown in (b) were conducted on the new CH_4 line. The gas flowed through the upstream part of the line at 0.8 SL/min and either bypassed the Sofnocat completely or flowed through only 1 part of the Sofnocat trap (the other part was replaced with an empty glass tube; see Figure 1); the gas was then delivered to the GC by a diaphragm pump. For testing part 1 of the trap, gas from an actual Pakitsoq air sample was used for a complete simulation of sample processing. For testing part 2, a synthetic high-CO gas mixture was used. The [CO] measurements were performed using a Hewlett Packard 5890 gas chromatograph with a reducing gas detector. The [CO] measurement blank was determined by running a CO-free gas through part 1 of the Sofnocat trap. All measurements are from single GC injections except where [CO] errors are given, in which case 3 injections were performed. The CO detector is not calibrated to measure concentrations much above ~100 ppb, and the response may not be completely linear.

Flow rate (SL/min)	Approx. gas residence time in Sofnocat (s)	[CO] before Sofnocat (ppb)	[CO] after Sofnocat (ppb)	[CH₄] before Sofnocat (ppb)	[CH₄] after Sofnocat (ppb)
2	0.35	693	3.4	426.5	426.5
2	0.35	7010	0	535.2	534.1
5	0.14	6872	0	533.8	534.6
2	0.35	6628	0	537.2	535.3
0.5	1.42	6603	0	534.9	537.0
0.1	7.09	6665	0	534.4	534.3

Table 1b See caption above.

	Bypassing Sofnocat: [CO] (ppb)	Through Sofnocat: [CO] (ppb)	[CO] error (ppb)
Part 1 of Sofnocat trap	2029	17.96	
Part 2 of Sofnocat trap	3300	16.15	1.45
[CO] measurement blank		16.89	0.89

One further concern was whether the 2 Russian doll cryogenic traps downstream of the Sofnocat were capable of quantitative removal of CO-derived CO_2. Brenninkmeijer (1993) described the use of Russian doll traps of very similar construction to ours for removing CO-derived CO_2. In his tests with a single trap containing 2 nested glass fiber thimbles with a 7 L/min flow rate, a 98% CO_2 removal efficiency was observed for a gas with [CO] of 20 ppb, and a 99.5% efficiency was observed for a gas with [CO] of 250 ppb. We take these values as a very conservative lower limit for the CO_2 trapping efficiency in our system, because our Russian doll traps contained 3 nested glass fiber thimbles rather than 2, our flow rate was much lower at 0.8 L/min, and our starting [CO] was much higher

at 800–2000 ppb, which should all result in better trapping than in the Brenninkmeijer (1993) tests. We then calculate that at the maximum possible ^{14}CO based on above measurements, the ^{14}C from CO which breaks through the Russian doll traps would amount to no more than 1.7% of the total ^{14}C from CH_4 in the samples. For $^{14}CH_4$ of ~30 pMC (typical for our samples), this would amount to an extra 0.5 pMC. However, as discussed above, this is almost certainly an overestimate.

Sample Yield and Mass-Dependent Fractionation

Sample yield and $\delta^{13}CH_4$ are important indicators of the CH_4 line performance and can be used to characterize mass-dependent fractionation during processing as well as to identify addition of extraneous carbon (e.g. from air leaks), both of which may affect measured sample $^{14}CH_4$. Sample yield is defined as (amount CO_2 actually recovered) / (amount CO_2 expected) × 100%. Sample yield and $\delta^{13}CH_4$ were monitored during testing and sample processing.

Yields for samples with [CH_4] of ~500 ppb were 93–95%, and slightly higher for samples with higher [CH_4]. $\delta^{13}CH_4$ tests with the CH_4 line (some shown in Table 2) indicated a slight mass-dependent fractionation, with $\delta^{13}C$ values decreasing from the true value with decreasing yield (and decreasing [CH_4]). Test results suggested that most of the fractionation resulted from incomplete CH_4 combustion in the furnace. However, some fractionation may have also been occurring during CO_2 trapping and transfer. Test 1 in Table 2 demonstrates that incomplete trapping of CO_2 downstream of the furnace results in a ^{13}C depletion in the trapped CO_2. ^{13}C depletion from incomplete CO_2 trapping has previously been observed by Brenninkmeijer and Röckmann (1996). The results of test 2 demonstrate that a sample ^{13}C depletion also occurs if a substantial portion of the sample is left behind in CO_2 transfer during the vacuum distillation.

Table 2 Tests of factors influencing the sample yield and isotopic fractionation in the new CH_4 conversion line. CH_4 line configuration and procedure were as described in the main text, with the following exceptions. In Test 1, only 1 LN_2-chilled trap was used to capture CO_2 downstream of the furnace instead of the usual 3. In Test 2, a ~20-µg aliquot of CO_2 with a known $\delta^{13}C$ was mixed with H_2O vapor from a previous sample run, and a CO_2 distillation was then performed as usual, except for the transfer into the manometer, which was cut short after 30 s (1 min too short). The fraction of sample left behind in the transfer was not quantified. In Test 4, 1 end of the sample gas cylinder sat in a bucket of ice; the pressures in the cylinder at the start and end of the run were 2.45 and 0.30 bar, respectively. In Test 6, the sample gas was bubbled through Milli-Q® water at a gas pressure of 1200 mbar prior to entering the CH_4 line. All tests listed are single sample runs, except for the controls (#3). All [CH_4] measurements were carried out using a Hewlett Packard 5890 gas chromatograph with a flame-ionization detector. $\delta^{13}C$ measurements were made using a Finnigan MAT 252 dual dynamic inlet isotope ratio mass spectrometer.

Test	[CH_4] (ppb)	Yield (%)	True $\delta^{13}CH_4$ (‰ PDB)	Measured $\delta^{13}C$ (‰ PDB)
1. Poor trapping of CO_2 downstream of furnace	517	69.1 ± 1.0	–47.23 ± 0.07	–48.83 ± 0.10
2. Incomplete transfer of CO_2	—	—	–47.02	–48.20 ± 0.10
3. Three control runs for tests 4–6 below	510	93.5 ± 0.2	–47.28 ± 0.15	–47.60 ± 0.03
4. Test gas run from a chilled cylinder down to low pressure	510	94.1 ± 1.0	–47.28 ± 0.15	–47.58 ± 0.08
5. Hydrocarbon-rich gas mixture	443	93.1 ± 1.0	—	—
6. Hydrocarbon-rich gas mixture saturated with H_2O vapor	443	92.7 ± 1.0	—	—

Overall, our tests demonstrated that although fractionation was occurring in the CH_4 line, its effect on the sample ^{14}C would be negligible compared to the overall $^{14}CH_4$ measurement uncertainty for Pakitsoq samples (~1 percent modern carbon (pMC)). For example, the maximum observed $\delta^{13}C$ shift due to processing fractionation for a ~500-ppb CH_4 sample was –0.6‰. A typical $^{14}CH_4$ value for the Greenland samples is ~30 pMC; assuming all the fractionation is mass dependent, this translates to a shift of –0.04 pMC in ^{14}C, or only 4% of the overall measurement uncertainty. $\delta^{13}CH_4$ was measured in the Greenland samples using GC-IRMS (Ferretti et al. 2005a) and some of the values have been reported in Schaefer et al. (2006). Because our ^{14}C AMS measurements used the sample ^{13}C beam as a reference, a CH_4 line fractionation correction was made to the measured Pakitsoq sample $\delta^{13}CH_4$ values based on the test results.

Tests of Breakthrough of Light Non-Methane Hydrocarbons

The Pakitsoq samples contained 1–6 ppb each of ethane (C_2H_6), ethene (C_2H_4), and ethyne (C_2H_2), as indicated by gas chromatography-mass spectrometry (GCMS) measurements (technique described in Mühle et al. [2007]). All the melt-extraction blanks contained less than 1 ppb of each of these, indicating that the light hydrocarbons originate mostly from the sample ice. Each of these compounds is volatile enough to possibly pass through LN_2-cooled traps in the upstream part of the CH_4 line and be combusted along with the sample CH_4 in the furnace. Since the ^{14}C of these C_2 hydrocarbons is unknown, this introduces a possible risk of contamination to the $^{14}CH_4$. To test whether any of the light C_2 hydrocarbons break through the upstream traps, a gas mixture containing 443 ppb of CH_4 and 114 ppb each of ethane, ethene, and ethyne, as well as 5 other light hydrocarbons was run through the line dry as well as with H_2O vapor added to better simulate the Pakitsoq samples. The results (Table 2) show no noticeable increase in the yield for either of these tests, and indicate that any ^{14}C interference from C_2 hydrocarbons is negligible. It is likely that the Sofnocat reagent plays a role in removing the C_2 hydrocarbons by oxidation to more condensable compounds, as the removal of C_2 and other hydrocarbons by Sofnocat was also observed by Ferretti et al. (2005b). Russian doll traps probably also play a role in the removal of C_2 hydrocarbons, as was observed by Brenninkmeijer (1991) and Pupek et al. (2005).

SAMPLE GRAPHITIZATION AND AMS MEASUREMENT

The CO_2 derived from CH_4 in the Pakitsoq samples was converted to graphite and measured by AMS at the Australian Nuclear Science and Technology Organisation (ANSTO). A full description of the ANSTO graphitization procedures can be found in Hua et al. (2004) and Smith et al. (2007). ANSTO operates 2 machines for AMS, the 10MV ANTARES accelerator (Fink et al. 2004) and the 2MV STAR accelerator, the latter manufactured by High Voltage Engineering Europa (HVEE). All Pakitsoq and test samples were measured on the ANTARES accelerator, utilizing the 4+ charge state, which gives a greater yield than the 3+ beams utilized on the STAR accelerator. Maximizing efficiency to produce the highest possible ^{14}C counting rate is essential for obtaining good measurement precision with low-^{14}C samples in the 20-µg range. Only the ^{13}C and the ^{14}C beams are normally measured on ANTARES, and the sample ^{14}C activity is corrected to the known $\delta^{13}C$ of the submitted sample.

Sample preparation procedures were modified from those given in Hua et al. (2004) in several ways in order to improve the graphitization rate, yield, and blank for small samples (10–45 µg C). First, the water vapor traps used with Pakitsoq samples consisted of an aluminum heat pipe immersed in a capped bath of ethanol and dry ice, giving cold trap temperatures of –60 to –70 °C during the graphitization reaction, as opposed to the standard ANSTO procedure of using Peltier chillers with a minimum temperature of –39 °C. Second, we used 1 mg of Sigma-Aldrich-400 (SA-400) 99.99+%

purity Fe powder catalyst for the reduction of CO_2 to graphite in the presence of hydrogen (H_2) instead of 1 mg of Cerac-325 Fe powder (99.9% purity). Third, we added the step of precleaning all flame-sealed Pyrex tubes containing sample CO_2 with ethanol and handled the tubes only with vinyl gloves. Fourth, the pumping time on the sample tubes prior to cracking the tubes on the vacuum line to release the sample CO_2 was increased from 1 to 5 min and a vacuum leak check step was added. Finally, a new system was developed for pressing the graphite from samples containing <500 µg C into aluminum cathodes. The standard ANSTO procedure for such samples involves front-pressing the Fe-graphite mixture with a pin and hammer into a 1-mm recess. This results in considerable variation in the depth of the sample surface below the cathode surface, depending on the amount of the Fe-graphite mixture pressed. There is also variation in resultant sample density and surface finish. Eliminating this variability with the new pressing system results in much improved and reproducible behavior of the sample in the ion source. A detailed description of this cathode pressing technique will be given elsewhere.

In the course of work on the Pakitsoq samples and associated tests, over 100 samples containing <45 µg C were processed using ~1 mg of SA-400 Fe powder as a catalyst and the described dry ice/ethanol cold trap. As a result of these procedural modifications, the graphitization reaction times for such small samples were decreased from 2.5 hr–4 days to 80 min for all samples. Such dramatic improvement in the reaction rates was shown to be due to the more efficient water vapor trapping (Smith et al. 2007).

The graphitization reaction yields were also improved, from 61–90% to 80–95% for samples containing 15–45 µg C. Prior tests (Smith et al. 2007) suggested that lower cold trap temperatures do not significantly affect the reaction yield; it is therefore most likely that the higher yields are due to the higher surface area of SA-400 than of Cerac-325 Fe catalyst. Improving graphitization yields was important because isotopic fractionation has been previously observed at ANSTO for samples with graphitization yields <85% (Hua et al. 2001); low yields also mean less available graphite for the AMS measurement. One graphite sample prepared using the new technique from 20 µg of CO_2, which had been derived from the oxalic-1 standard (OX-1), was measured for $\delta^{13}C$ by elemental analyzer-isotope ratio mass spectrometry (EA-IRMS). This sample had a graphitization yield of 82.7% and gave a $\delta^{13}C$ of –20.0‰. The consensus $\delta^{13}C$ value of OX-1 is –19.3‰ (Stuiver 1983). This suggests that the amount of isotopic fractionation during graphitization of small samples with the new technique is small. This is further confirmed by the ^{14}C results on small test samples presented below.

Because of the low ^{14}C activity (~30 pMC) and the small size of the Pakitsoq samples (most between 15–25 µg C), minimizing the ^{14}C processing blanks was of key importance. Earlier determination of the graphitization blank at ANSTO (Hua et al. 2001) found an extraneous carbon mass of 0.14 ± 0.02 µg if a ^{14}C activity of 100 pMC is assumed. Our tests (see section "Corrections for Processing Blank and Fractionation at ANSTO") show that with the modified procedure this blank has been reduced to 0.03 µg of 100 pMC carbon. Although no tests were conducted to investigate the effect of each procedural modification on the blank by itself, it is likely that the most important factor in reducing the blank was the use of the very high purity (99.99+%) SA-400 Fe catalyst.

^{14}C RESULTS FOR STANDARDS AND PROCESS BLANKS AND ^{14}C CORRECTIONS

The General Correction Method and ^{14}C Units Used

The Greenland $^{14}CH_4$ samples underwent 4 major stages of handling, each of which is likely to be associated with the addition of extraneous carbon and/or isotopic fractionation. First, the ancient air

trapped in glacial ice was obtained by the means of a vacuum melt-extraction in the field (Petrenko et al. 2008). Second, the CH_4 in this air was combusted and the resulting CO_2 collected. Third, the sample CO_2 was converted to graphite. Finally, the ^{14}C was measured by AMS. The simulated gas extractions, conducted in Greenland along with the actual air extractions from ice, were performed using a single standard gas mixture containing ~500 ppb CH_4 in uhp air. These simulated extractions did not therefore mimic the full range of [CH_4] found in our real samples (~400–800 ppb), and cannot be used to accurately assess the overall ^{14}C blank for all stages of sample handling. It is therefore necessary to assess each of these handling blanks separately.

Assuming that the effects of isotopic fractionation for each processing step are known or insignificant (see further discussion of this below), the general approach for correcting sample ^{14}C is as follows:

$$M_{\text{final}}\,^{14}C_{\text{final}} \;=\; M_{\text{true}}\,^{14}C_{\text{true}} + M_{\text{extr}}\,^{14}C_{\text{extr}} \tag{1}$$

where M_{final} and $^{14}C_{\text{final}}$ are the carbon mass and ^{14}C specific activity of the processed sample, M_{true} and $^{14}C_{\text{true}}$ are the true carbon mass and ^{14}C specific activity of the unprocessed sample and M_{extr} and $^{14}C_{\text{extr}}$ are the carbon mass and ^{14}C specific activity of the extraneous carbon added during processing.

To stay consistent with prior work on atmospheric $^{14}CH_4$ (Wahlen et al. 1989; Lassey et al. 2007), we use the units of percent modern carbon (pMC) for reporting our results and making corrections to ^{14}C for extraneous carbon added during processing. As accepted at the 8th International Conference on Radiocarbon Dating, pMC is defined as:

$$\text{pMC} \;=\; \frac{A_{\text{SN}}}{A_{\text{ON}}} \times 100 \tag{2}$$

(Stuiver and Polach 1977). Here, A_{ON} is the normalized ^{14}C activity of the oxalic-1 standard (OX-1), and A_{SN} is the normalized ^{14}C activity of the sample, both also as defined in Stuiver and Polach (1977).

The pMC unit is not exactly mass-additive in the sense defined by Equation 1 because it is not a specific activity. It is, however, approximately mass-additive. For the very small levels of extraneous carbon added during the processing of Pakitsoq samples (<0.4 µg, see discussion below), the errors in ^{14}C correction calculations arising from using the pMC units amount to <0.3% of sample ^{14}C value, or <0.1 pMC for samples with [14]C = 30 pMC (typical for Pakitsoq samples). As these errors are at least an order of magnitude smaller than the typical overall ^{14}C uncertainties after all corrections (~1.0 pMC), we find the pMC unit acceptable to use in the calculation of corrections.

Corrections for Processing Blank and Fractionation at ANSTO

Thirty-six blank and standard samples were measured to assess the fractionation and blank from processing at ANSTO (Table 3). Small (10, 20, and 40 µg C) samples of blanks and standards were decanted from larger parent CO_2 samples (~220 to ~10,000 µg C) without affecting the sample ^{14}C through mass-dependent fractionation (see Table 3 caption), and both the small and parent samples were graphitized and measured for [14]C. As can be seen from the table, the agreement between the small samples and the larger parent samples is very good for all samples and often within the measurement errors. For the blank samples, if we assume that the average of the 4 large blanks represents the true ^{14}C of the marble (0.15 pMC), then the average of the four ~10-µg blank samples (0.43 pMC) is only shifted by 0.28 pMC from the true value.

Table 3 Samples processed to assess the ANSTO procedural blank. All masses were determined volumetrically prior to graphitization. For the marble blanks, CO_2 was evolved with 85% phosphoric acid from a single grain of IAEA C1 marble and subsequently decanted through a metal bellows valve to make the individual samples listed in the table. For IAEA-C8, a ~500-µg sample was split into one 460-µg and two ~20-µg samples by allowing the CO_2 to equilibrate between flasks in a vacuum line. The small OX-1-derived CO_2 samples and SIO 30 pMC CO_2 samples were prepared in a similar manner, with the 440-µg sample being the parent of all the ~20-µg samples, and the 220-µg sample being the parent of all the ~10-µg samples for OX-1, and the 560-µg sample being the parent of all small 30-pMC samples. The pMC value assigned to the average of all large OX-1 standards is 103.98. Samples that went through graphitization reactor 1 were treated separately when making ^{14}C corrections.

Sample type	Graphitization reactor(s)	n	Average mass (µg C)	Larger of average mass uncertainty or stdev (µg C)	Average ^{14}C (pMC)	Larger of ^{14}C average uncertainty or stdev for the set (pMC)
Marble blank	2,3	4	1510	20	0.15	0.04
Marble blank	2,3,5	3	39.63	0.43	0.22	0.04
Marble blank	1	1	39.59	0.43	0.48	0.09
Marble blank	5	2	19.71	0.21	0.42	0.05
Marble blank	1	2	20.03	0.22	1.08	0.16
Marble blank	2,3	4	9.87	0.15	0.43	0.09
IAEA-C8	1	2	2000	30	15.33	0.21
IAEA-C8	2	1	460	10	15.53	0.17
IAEA-C8	2,3	2	21.28	2.83	16.03	0.37
SIO 30 pMC CO_2	5	1	560	10	31.13	0.28
SIO 30 pMC CO_2	2,3,5	3	20.06	0.46	30.75	0.63
SIO 30 pMC CO_2	1	1	20.63	0.22	31.37	0.35
Large OX-1 avg			2000		103.98	
OX-1	5	1	440	10	102.76	0.64
OX-1	1	1	220	10	104.70	0.51
OX-1	2,3,5	3	22.06	1.48	103.68	1.85
OX-1	1	1	21.64	0.23	104.78	0.95
OX-1	2,3	4	11.86	0.76	105.07	1.50

This indicates a remarkably low ^{14}C blank. For example, assuming that the ^{14}C of the contaminant is 100 pMC, its mass is 0.03 µg. This low level of extraneous carbon and the fact that previous ANSTO work has demonstrated that no significant isotopic fractionation takes place for graphitization of samples ≥100 µg C (Hua et al. 2001), allows us to assume that the large "parent" samples represent the true ^{14}C values and determine the blank corrections based on the observed shifts between the parent and small samples. Graphitization reactor 1 had a higher blank than the other reactors used (Table 3); this was further confirmed by the uncorrected ^{14}C observed in CH_4 line and Greenland melt-extraction processing blanks (not shown). We therefore treated reactor 1 separately in determining the ^{14}C corrections.

A further observation can be made when comparing the measured ^{14}C activities of the small (~10 and ~20 µg) OX-1 standards with the larger (220 and 440 µg, respectively) "parent" OX-1 standards (Table 3 and caption). Except for small samples that went through graphitization reactor 1, there is excellent agreement within measurement uncertainty between the small and parent samples. Considering that the amount of extraneous carbon added during processing is very small, this indicates that any isotopic fractionation resulting from processing is not affecting the ^{14}C of small samples significantly. However, we still take the possible effects of fractionation from processing at ANSTO into account when making corrections to sample ^{14}C, as is shown below.

Assuming that $M_{final} = M_{true} + M_{extr}$, Equation 1 above can be re-arranged to yield:

$$({}^{14}C_{final} - {}^{14}C_{true})M_{true} = -{}^{14}C_{final}M_{extr} + {}^{14}C_{extr}M_{extr} \tag{3}$$

In this case, M_{final} and $^{14}C_{final}$ refer to the graphite sample as measured on the accelerator. Fractionation has negligible effects for blank samples, so the only process by which their ^{14}C can be shifted is addition of extraneous carbon. We know $^{14}C_{true}$ from the measurements on the (large) parent samples; M_{true} is also known for all samples. If $({}^{14}C_{final} - {}^{14}C_{true}) \times M_{true}$ is plotted against $^{14}C_{final}$, the slope should be $-M_{extr}$ and the intercept $^{14}C_{extr} \times M_{extr}$, so the mass and ^{14}C of the extraneous carbon added during processing can in principle be determined. When this is done for all blanks except those processed in reactor 1, however (plot not shown), a positive slope results, suggesting a negative M_{extr}, which has no physical meaning. We suspect that this may be due to the relatively small number of blanks measured for each mass, which results in under-sampling of the full ^{14}C variability for the blanks and deviations in the calculated mean ^{14}C for each mass from the true mean.

All the blank and standard samples must therefore be considered together to determine the ^{14}C corrections for ANSTO processing. This complicates the situation somewhat because for non-blank samples, isotopic fractionation during graphitization, as well as during the accelerator measurement, may also have an effect on [14]C. The effect of isotopic fractionation alone on the ^{14}C of the processed sample will be proportional to the ^{14}C content of the sample:

$$^{14}C_{processed} = \alpha_0 \, {}^{14}C_{initial} \tag{4}$$

Here, α_0 is a fractionation coefficient. In our case, the mass of the small samples is variable; since larger fractionation had previously been observed at ANSTO for smaller samples (Hua et al. 2001), a good first-order approximation is that the effect of fractionation is inversely proportional to mass. This can be parameterized as follows:

$$^{14}C_{processed} = \left(1 + \frac{\alpha}{M_{true}}\right){}^{14}C_{initial} \tag{5}$$

In this case, α is a constant fractionation coefficient that has units of mass. To combine the effects of fractionation and addition of extraneous carbon, we need to make some assumptions regarding whether the fractionation happens before or after the extraneous carbon is added (or both). However, considering that the amount of extraneous carbon and its effects on the ^{14}C are clearly very small, this choice will have negligible effects on the ^{14}C correction. We will therefore assume that all fractionation happens after the extraneous carbon is added. Solving Equation 3 for $^{14}C_{final}$ and adding the effect of fractionation as parameterized in Equation 5, we get:

$$^{14}C_{final} = \left(1 + \frac{\alpha}{M_{true}}\right)\frac{^{14}C_{true}M_{true} + {}^{14}C_{extr}M_{extr}}{M_{true} + M_{extr}} \tag{6}$$

Multiplying through by $(M_{true} + M_{extr})$ and expanding all the terms gives:

$$^{14}C_{final}M_{true} + {}^{14}C_{final}M_{extr} =$$

$$^{14}C_{true}M_{true} + {}^{14}C_{extr}M_{extr} + \frac{\alpha}{M_{true}}{}^{14}C_{true}M_{true} + \frac{\alpha}{M_{true}}{}^{14}C_{extr}M_{extr} \tag{7}$$

Based on how close measurements of both the blank and standard samples were to true ^{14}C values, we know that both the mass of extraneous carbon and the effect of fractionation on ^{14}C must be quite small, meaning that $M_{extr} \ll M_{true}$ as well as $\alpha \ll M_{true}$. The last term in Equation 7 is therefore negligible compared to the others, and the equation simplifies to:

$$^{14}C_{final}M_{true} + {}^{14}C_{final}M_{extr} = {}^{14}C_{true}M_{true} + {}^{14}C_{extr}M_{extr} + \alpha{}^{14}C_{true} \tag{8}$$

The $\alpha{}^{14}C_{true}$ term can be expanded to $\alpha{}^{14}C_{final} + \alpha({}^{14}C_{true} - {}^{14}C_{final})$. Because both α and $({}^{14}C_{true} - {}^{14}C_{final})$ are very small, the term $\alpha({}^{14}C_{true} - {}^{14}C_{final})$ is negligible compared to the other terms in Equation 8. The equation can then be rewritten as

$$^{14}C_{final}M_{true} + {}^{14}C_{final}M_{extr} = {}^{14}C_{true}M_{true} + {}^{14}C_{extr}M_{extr} + \alpha{}^{14}C_{final} \tag{9}$$

Further re-arranging yields

$$M_{true}({}^{14}C_{final} - {}^{14}C_{true}) = {}^{14}C_{final}(\alpha - M_{extr}) + {}^{14}C_{extr}M_{extr} \tag{10}$$

M_{true}, $^{14}C_{final}$, and $^{14}C_{true}$ are known, so $M_{true}({}^{14}C_{final} - {}^{14}C_{true})$ can now be plotted against $^{14}C_{final}$ and a linear least-squares fit applied to find the slope $(\alpha - M_{extr})$ and the intercept $^{14}C_{extr}M_{extr}$.

Figure 2 shows these plots for all the blanks and standards processed through graphitization reactors 2, 3, and 5 (a) as well as for those processed through reactor 1 (b). Surprisingly, the slopes are positive, suggesting that $\alpha > M_{extr}$ and that there is a ^{14}C-enriching fractionation. We speculate that this may result from fractionation in the accelerator, since fractionation during graphitization results in a ^{14}C depletion. Knowing the slope and the intercept, the correction applied to determine the true ^{14}C prior to ANSTO processing is

$$^{14}C_{true} = {}^{14}C_{final} - \frac{^{14}C_{final} \times \text{slope} + \text{intercept}}{M_{true}} \tag{11}$$

The effect of these corrections is small and is illustrated for 2 samples in Table 6.

Corrections for CH_4 Extraction Line Blank

Effects of mass-dependent fractionation on ^{14}C during the CH_4 combustion and separation from the air stream were shown above to be negligible for the Greenland samples; we therefore do not consider fractionation in determining the corrections for this stage of sample processing. There are, however, 2 possible mechanisms by which extraneous carbon can be added. The first is independent of the time it takes to run the air sample through the CH_4 extraction line; we will refer to the ^{14}C and
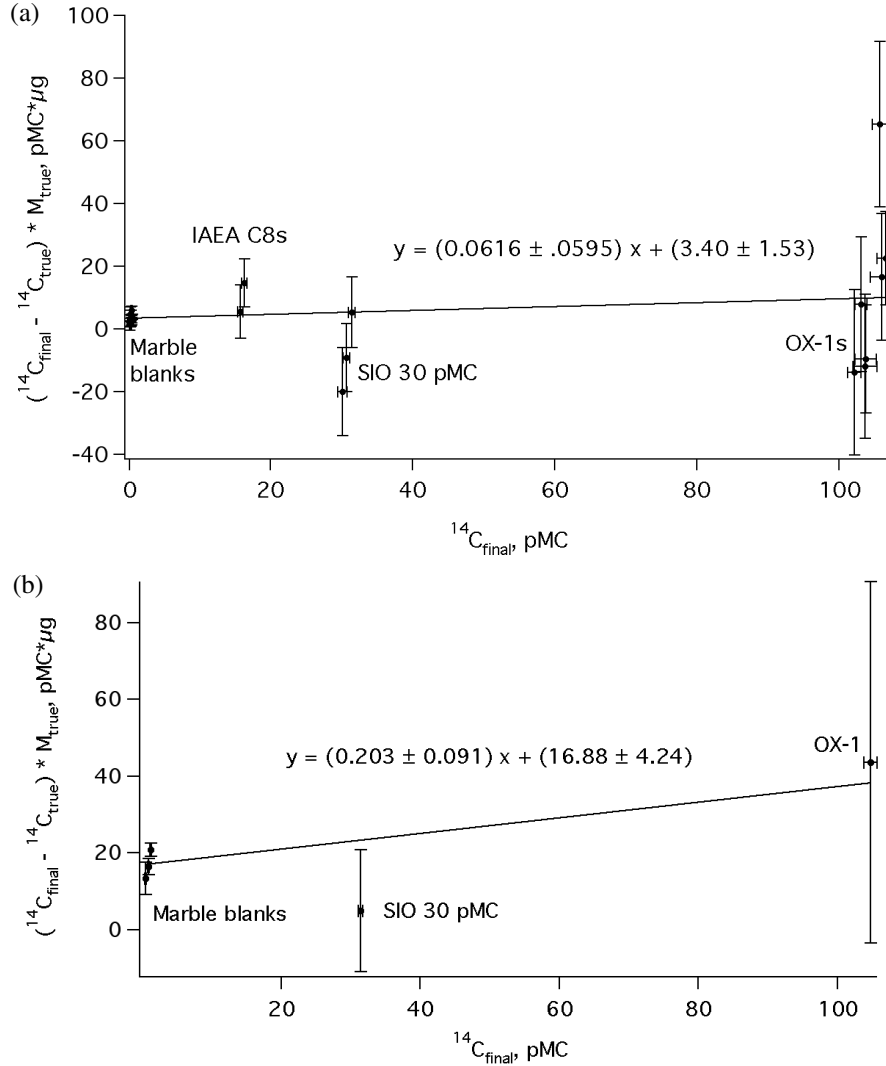
Figure 2 Plots of $M_{true}(^{14}C_{final} - ^{14}C_{true})$ versus $^{14}C_{final}$ for ANSTO blanks and standards processed through reactors 2, 3, and 5 (a) and 1 (b). Data for all individual samples are plotted. Errors for data points are as determined by error propagation. Least-squares line fits to the data with equations are shown. The intercept for each equation was set to the average $M_{true}(^{14}C_{final} - ^{14}C_{true})$ for the blanks, and the intercept error is taken as the standard deviation of $M_{true}(^{14}C_{final} - ^{14}C_{true})$ values for the blanks. The errors shown for the slopes are 1 standard deviation.

mass of this type of extraneous carbon as $^{14}C_{fixed}$ and M_{fixed} and assume that both of these are constant. An example of this would be extraneous carbon added during the flame-sealing step. The second mechanism involves gradual addition of extraneous carbon with a ^{14}C activity of $^{14}C_{time}$ over time t at a rate of R µg/min. Examples of this are carbon from CO_2 in ambient air from leaks and gradual outgassing of CO_2 from the CH_4 line components. The mass ratio of extraneous carbon to sample CH_4 carbon for this second process will be inversely proportional to $[CH_4]$ of the air sample. The relationship between the $^{14}C_{final}$ post-processing and $^{14}C_{true}$ pre-processing can then be written as:

$$^{14}C_{final}M_{final} = {}^{14}C_{true}M_{true} + {}^{14}C_{fixed}M_{fixed} + {}^{14}C_{time}Rt \qquad (12)$$

Here, $^{14}C_{final}$ is the ^{14}C with ANSTO processing corrections applied, and M_{final} is as determined at ANSTO prior to graphitization.

Table 4 gives a summary of the samples run to determine the CH_4 line procedural blank. As can be seen from the ^{14}C (corrected for ANSTO processing blank), the CH_4 line blanks are also very low, with very good agreement between large, high-[CH_4] samples and small, low-[CH_4] samples for which the CH_4 originated from the same air tank (Table 4 caption). In principle, the fixed and time-dependent components of extraneous carbon added can be determined by comparing the ^{14}C results between the sample sets shown. However, precise determination of the process blank is complicated by the fact that the magnitude of the ^{14}C differences between sets of samples containing identical CH_4 (all the ^{14}C-dead samples; all the modern samples) are similar to the ^{14}C uncertainties. A further complication is an outlier with a high ^{14}C in the 1000-ppb ^{14}C-dead set (1.08 pMC, as compared to an average of 0.24 pMC for the other 3 samples in that set), for which we have no explanation. Nevertheless, a blank correction can still be determined as long as some simplifying assumptions are made. We first consider the two 500-ppb [CH_4] sets. These samples were all of approximately the same carbon mass (as measured immediately prior to graphitization), so M_{final} is the same. Because their [CH_4] is also the same, the $^{14}C_{time}$ Rt term is the same for both sets. $^{14}C_{fixed}$ and M_{fixed} are both constant; this also means that the total amount of extraneous carbon added is the same for both sets and M_{true} is the same. Writing out Equation 12 for both 500-ppb sets and subtracting the 2 equations, we get:

$$(^{14}C_{final\ modern} - {}^{14}C_{final\ \text{``dead''}})M_{final} = (^{14}C_{true\ modern} - {}^{14}C_{true\ \text{``dead''}})M_{true} \qquad (13)$$

because all the extraneous carbon terms cancel. Because the blanks are clearly small, we take $^{14}C_{true\ \text{``dead''}}$ as the ^{14}C of the large 28-ppm [CH_4] sample set. In the same manner, $^{14}C_{true\ modern}$ can be approximated by the ^{14}C of the large 1750-ppb sample set. In this way, the M_{true}/M_{final} can be determined and from that the overall mass of extraneous carbon is found to be 0.23 ± 0.16 µg. The overall ^{14}C of extraneous carbon can then be calculated by applying Equation 1 to the 500-ppb ^{14}C-dead set, obtaining 23.57 ± 16.22 pMC.

Table 4 A summary of the blank and modern samples processed to assess the CH_4 extraction line blank, using the procedure described in the text. The "ppb" and "ppm" (parts per million) refer to [CH_4] of the gases used. The 500-ppb and 1000-ppb "^{14}C-dead" gases were prepared by diluting the 28-ppm gas with CH_4-free air and should thus have the same ^{14}C. The gas used for "large" and "small" modern sets was clean ambient air from the same tank, collected at Baring Head, New Zealand. The "500 ppb modern" gas was made by diluting air from this same tank with CH_4-free air. Run time is the total time for collection of CO_2 downstream of the CH_4 combustion furnace. Sample masses are as determined at ANSTO immediately prior to graphitization. The listed ^{14}C values have been corrected for the ANSTO processing blank as described in the text.

Sample type	n	Average sample mass (µg C)	Larger of average mass uncertainty or stdev of the set (µg C)	Average run time (min)	Run time stdev (min)	Average ^{14}C corrected for ANSTO blank (pMC)	Larger of ^{14}C average uncertainty or stdev of the set (pMC)
Large 28 ppm ^{14}C-dead	3	190	10	16.51	0.01	0.22	0.04
1000 ppb ^{14}C-dead	4	19.39	0.37	45.11	0.23	0.45	0.42
500 ppb ^{14}C-dead	4	19.07	0.45	91.48	0.90	0.50	0.08
500 ppb modern	4	19.07	0.67	90.17	0.20	130.54	1.40
Small 1750 ppb modern	4	19.76	0.32	26.43	0.30	132.48	1.58
Large 1750 ppb modern	3	129.50	0.80	180.88	1.50	131.87	0.62

A further simplification can be made when considering the relative importance of the fixed and time-dependent components of extraneous carbon addition. The large and small 1750-ppb [CH_4] modern sets show excellent agreement in their ^{14}C. The time-dependent component would be the same for these 2 sets, so only the fixed component would produce differences in the ^{14}C. When comparing the 500-ppb modern and small 1750-ppb modern sets, however, the fixed component would not produce a difference in the ^{14}C because the sample mass is the same for these 2 sets. Here, the ^{14}C shows a larger difference between the sets, however, and only the time-dependent component can explain it. We therefore make the assumption that the fixed component is negligible and that all of the extraneous carbon is added in a time-dependent fashion. Equation 12 then simplifies, and given that now $M_{final} = M_{true} + Rt$, it can be rearranged to yield:

$$\frac{(^{14}C_{true} - {}^{14}C_{final})M_{true}}{t} = {}^{14}C_{final}R - {}^{14}C_{time}R \tag{14}$$

The expression on the left side can now be plotted against $^{14}C_{final}$. Because the amount of extraneous carbon added is very small, the mass as determined prior to graphitization provides a good estimate of M_{true} for the purposes of this plot; $^{14}C_{true}$ for the dead samples is known from the 28-ppm set, and can be estimated for the modern samples from the large 1750-ppb set. This plot for all the ~20-µg samples is shown in Figure 3. From the slope and intercept, $R = 0.00188 \pm 0.00153$ µg/min and $^{14}C_{time} = 42.16 \pm 72.96$ pMC. The large uncertainty in the intercept and $^{14}C_{time}$ arises from the surprisingly high ^{14}C of one of the 1000-ppb samples.
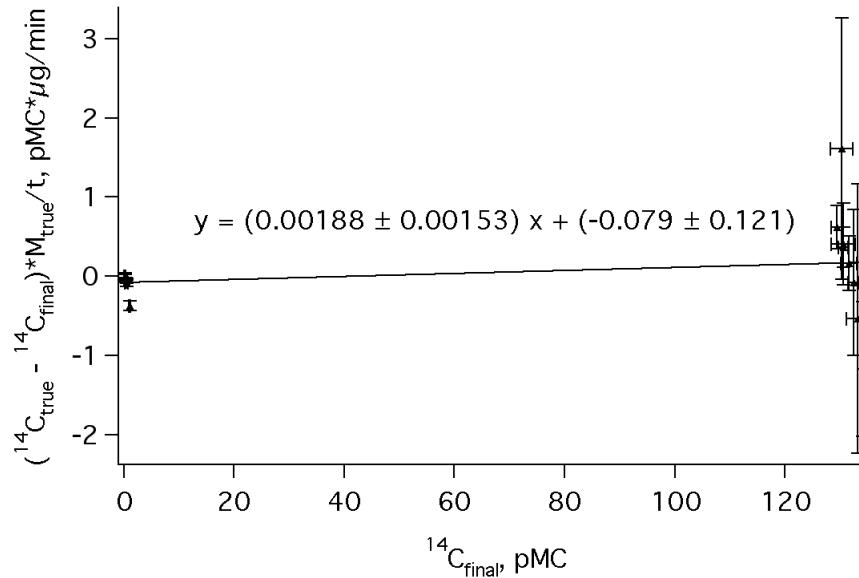

Figure 3 Determination of the NIWA processing blank from all individual ~20-µg samples. The least-squares linear fit with equation is shown. The intercept is fixed at the average value of ($^{14}C_{true} - {}^{14}C_{final}$) × M_{true}/t for all the ^{14}C-dead samples; the uncertainty in the intercept is the standard deviation of all these values. The error shown for the slope is 1 standard deviation.

Corrections to sample ^{14}C for CH_4 line processing are made according to:

$$^{14}C_{true} = \frac{(^{14}C_{final}M_{final} - ^{14}C_{time}Rt)}{M_{final} - Rt} \tag{15}$$

The effect of these corrections for 2 of the Pakitsoq samples can be seen in Table 6; sample ^{14}C changes very little as a result, but the uncertainties increase substantially.

^{14}C Corrections for Greenland Melt-Extractions

The air for paleo-$^{14}CH_4$ analyses was obtained from large volumes of ancient glacial ice outcropping on the ice sheet margin in West Greenland, and the details are presented in Petrenko et al. (2008). Briefly, glacial ice was melted under vacuum in the field, and the released ancient air transferred to storage cylinders. Two to 3 melt-extractions were performed to obtain air for each sample. Simulated gas extractions were conducted to mimic the effects of this procedure on sample ^{14}C and $[CH_4]$. A mixture of 500-ppb CH_4 in uhp air was used in the simulated extractions ("CH_4 standard gas" in Table 5), and separate blank extractions were conducted for each type of actual sample taken, as illustrated in Table 5. The blank extractions were conducted in such a way that the combined amount of extraneous carbon added for all blank extractions should have been equal to that for all the actual melt-extractions for a particular type of sample (e.g. Oldest Dryas blanks and Oldest Dryas samples) (Petrenko et al. 2008).

Table 5 Summary of samples processed to assess the field melt-extraction blank for each type of actual Pakitsoq ancient air sample. "CH_4 standard gas" was used in all the simulated extractions. All $[CH_4]$ measurements were conducted at NIWA using a Hewlett Packard 5890 gas chromatograph with a flame-ionization detector. Average ^{14}C uncertainties for the sample sets (after ANSTO and CH_4 line corrections were applied) are listed instead of ^{14}C standard deviations of the sets because the former are larger.

Sample type	n	Average ^{14}C corrected for ANSTO and CH_4 line blanks (pMC)	Average ^{14}C uncertainty for the set (pMC)	Corrected average mass (µg C)	Mass stdev (µg C)	[CH4] (ppb)	[CH4] error (ppb)
CH_4 standard gas	4	–0.02	0.60	19.05	0.26	500.41	0.84
Preboreal Blank	2	–0.09	0.61	19.03	0.14	502.82	0.38
Transition Blank	2	0.01	0.58	19.03	0.27	501.67	0.74
Younger Dryas Blank	2	–0.12	0.60	18.63	0.30	502.01	0.16
Bølling Blank	2	0.48	0.56	20.84	1.51	502.99	0.42
Oldest Dryas Blank	2	0.08	0.56	20.23	0.81	503.63	0.79

As can be seen from comparing the $^{14}CH_4$ of the CH_4 standard gas (corrected for ANSTO and CH_4 line blanks) with that of the extraction blanks (Table 5), the effect on ^{14}C of extraneous carbon added during the melt-extractions is not significant given the uncertainties. Comparison of $[CH_4]$ in the extraction blanks with the $[CH_4]$ of the standard gas shows that the extraneous carbon comprises <0.7% of the total sample carbon in all cases. Despite the very small observed effects on ^{14}C, we use the data from the extraction blanks to further correct the ^{14}C of the actual samples. Measurements of $\delta^{18}O$ of O_2 and $\delta^{15}N$ of N_2 in the Pakitsoq samples demonstrated that the melt-extraction does not result in significant gas-isotopic fractionation (Petrenko et al. 2008), so only effects of extraneous carbon on ^{14}C need to be considered as presented in Equation 1. M_{extr} is easily determined for each

type of sample from the [CH_4] offsets between the extraction blanks and the CH_4 standard. The true ^{14}C of the CH_4 standard gas is taken to be 0 pMC based on the ^{14}C results with ANSTO and CH_4 line corrections included, which makes for straightforward determination of [14]C_{extr} for each type of sample. The true [14]CH_4 of the air present in the sampled ice is then determined from

$$^{14}C_{true} = \frac{^{14}C_{final}M_{final} - {}^{14}C_{extr}M_{extr}}{M_{final} - M_{extr}} \tag{16}$$

Here, [14]C_{final} is the ^{14}C with ANSTO and CH_4 line corrections incorporated, and M_{final} is the mass as measured prior to graphitization and corrected for extraneous carbon added in the CH_4 extraction line.

The [14]CH_4 results for the actual Greenland samples will be presented elsewhere. However, to illustrate the effect of the stepwise ^{14}C corrections we show the results for the 2 Oldest Dryas samples in Table 6. As can be seen, the corrections are small for each of the processing steps, with the ^{14}C uncertainties growing with each correction.

Table 6 The effect of progressive ^{14}C corrections for each processing step on 2 of the actual Pakitsoq samples.

Sample	Uncorrected [14]CH_4 (pMC)	Error (pMC)	Graphitization reactor	Corrected for ANSTO blank (pMC)	Error (pMC)	Further corrected for CH_4 line blank (pMC)	Error (pMC)	[14]CH_4 FINAL (further corrected for melt-extraction blank) (pMC)	Error (pMC)
Oldest Dryas 1	28.54	0.44	5	28.29	0.45	28.17	0.88	28.26	1.06
Oldest Dryas 2	29.71	0.38	1	28.71	0.44	28.59	0.87	28.69	1.05

SUMMARY AND CONCLUSIONS

A new method has been developed for measurements of [14]CH_4 in ancient air samples obtained from glacial ice. A new CH_4 conversion line was constructed and tested extensively to minimize the [14]CH_4 processing blank. Our tests indicated that the mass and ^{14}C activity of extraneous carbon added during the combustion and separation of CH_4 from the air stream were 0.23 ± 0.16 µg and 23.57 ± 16.22 pMC for ~20-µg C, 500-ppb [CH_4] samples. This represents a dramatic improvement over our early attempts at processing small, ~500-ppb [CH_4] samples when the mass of extraneous carbon added was up to 2.6 µg if ^{14}C activity of 100 pMC is assumed. The new CH_4 line utilizes a small amount (~1 g) of platinized quartz wool for CH_4 combustion, as opposed to a much larger amount (~200 g) of platinized alumina used for the same purpose in the pre-existing CH_4 line. The lower ^{14}C blank and no detectable carbon sample memory in the new line are most likely a result of less carbon being adsorbed onto the much lower overall surface area of the platinized quartz wool catalyst. It has recently been shown that palladized quartz wool is even more effective at CH_4 conversion than platinized quartz wool, and yields lower carbon blanks with CH_4 isotopic analyses of small atmospheric samples (Fisher et al. 2006). Palladized quartz wool would therefore also be a good choice for future paleo-[14]CH_4 work. Keeping the line and combustion furnace under high vacuum when not in use probably results in a further lowering of the ^{14}C blank. Very high [CO] in the Greenland air samples, of concern because of potentially high [14]CO, was quantitatively removed using the Sofnocat reagent. In addition, it was demonstrated that there are no significant effects on sample [14]CH_4 from mass-dependent fractionation or interference from non-methane light volatile organic compounds (VOCs) in the CH_4 conversion line.

Extensive testing and method development was also carried out at ANSTO to overcome the problem of unusually long (2–4 days) graphitization times for some small samples as well as to further reduce the processing ^{14}C blank. Graphitization times have been reduced to 1 hr or less for all samples <25 µg C, with the most important factor being a colder trap for more efficient H_2O vapor trapping during the reaction. The amount of extraneous carbon added during graphitization (if assumed to have a ^{14}C activity of ~100 pMC) has been reduced to 0.03 µg, which is unprecedented to the best of our knowledge. The most important factor in reducing the blank was likely the use of ultra-high-purity Sigma-Aldrich-400 Fe powder catalyst, though the development of a new cathode pressing system and increased care taken with each individual sample during processing probably also contributed.

Test results indicate that the amount of extraneous carbon added during the melt-extraction of air from ancient glacial ice in Greenland was comparably low. The average uncorrected ^{14}C for all the Greenland melt-extraction blank samples (all ~500 ppb CH_4, ~20 µg C, ^{14}C-dead to begin with) was 0.75 pMC, which represents a cumulative blank for overall sample processing. Such low blanks, as well as our demonstrated ability to make meaningful ^{14}C corrections for each step of the processing, give us confidence in being able to accurately determine the $^{14}CH_4$ of the ancient air in sampled glacial ice. $^{14}CH_4$ in the Pakitsoq ancient air samples has been successfully measured, and the results, which will be presented elsewhere, may provide constraints on the fossil fraction of paleo-CH_4 budgets, as well as further insight into the potential role of methane clathrates in rapid CH_4 increases during the last deglaciation.

The methods developed for CH_4 extraction from relatively small, low-[CH_4] and low-$^{14}CH_4$ air samples will be useful for future paleo-$^{14}CH_4$ work and may also find applications in modern atmospheric $^{14}CH_4$ monitoring. The methods developed for AMS preparation and measurement of very small, low-^{14}C activity CO_2 samples are likely to find broader paleoenvironmental and geochronological applications.

ACKNOWLEDGMENTS

REFERENCES

Brasseur GP, Orlando JJ, Tyndall GS, editors. 1999. *Atmospheric Chemistry and Global Change*. New York: Oxford University Press. 654 p.

Brenninkmeijer CAM. 1991. Robust, high-efficiency, high-capacity cryogenic trap. *Analytical Chemistry* 63(11):1182–4.

Brenninkmeijer CAM. 1993. Measurement of the abundance of ^{14}CO in the atmosphere and the $^{13}C/^{12}C$ and $^{18}O/^{16}O$ ratio of atmospheric CO with applications in New Zealand and Antarctica. *Journal of Geophysical Research* 98(D6):10,595–614.

Brenninkmeijer CAM, Röckmann T. 1996. Russian doll type cryogenic traps: improved design and isotope separation effects. *Analytical Chemistry* 68(17):3050–3.

Brook EJ, Harder S, Severinghaus J, Steig EJ, Sucher

CM. 2000. On the origin and timing of rapid changes in atmospheric methane during the last glacial period. *Global Biogeochemical Cycles* 14(2):559–72.

Buffett B, Archer D. 2004. Global inventory of methane clathrate: sensitivity to changes in the deep ocean. *Earth and Planetary Science Letters* 227(3–4):185–99.

Chappellaz J, Bluniert T, Raynaud D, Barnola JM, Schwander J, Stauffer B. 1993. Synchronous changes in atmospheric CH$_4$ and Greenland climate between 40 and 8 kyr BP. *Nature* 366(6454):443–5.

Colussi AJ, Hoffmann MR. 2003. In situ photolysis of deep ice core contaminants by Cerenkov radiation of cosmic origin. *Geophysical Research Letters* 30(4): 1195, doi:10.1029/2002GL016112.

Conny JM, Currie LA. 1996. The isotopic characterization of methane, non-methane hydrocarbons and formaldehyde in the troposphere. *Atmospheric Environment* 30(4):621–38.

Etheridge DM, Steele LP, Francey RJ, Langenfelds RL. 1998. Atmospheric methane between 1000 AD and present: evidence of anthropogenic emissions and climatic variability. *Journal of Geophysical Research* 103(D13):15,979–93.

Ferretti DF, Miller JB, White JWC, Etheridge DM, Lassey KR, Lowe DC, MacFarling Meure CM, Dreier MF, Trudinger CM, van Ommen TD, Langenfelds RL. 2005a. Unexpected changes to the global methane budget over the past 2000 years. *Science* 309(5741): 1714–7.

Ferretti D, Fraser A, Lassey K, Martin R, Brailsford G, McGregor J. 2005b. Using electrical sensors to estimate methane emissions from farm animals. Paper presented at the Meteorological Society of New Zealand Annual Conference. Wellington, New Zealand.

Fink D, Hotchkis M, Hua Q, Jacobsen G, Smith AM, Zoppi U, Child D, Mifsud C, van der Gaast H, Williams A, Williams M. 2004. The ANTARES AMS facility at ANSTO. *Nuclear Instruments and Methods in Physics Research B* 223–224:109–15.

Fisher R, Lowry D, Wilkin O, Sriskantharajah S, Nisbet EG. 2006. High-precision, automated stable isotope analysis of atmospheric methane and carbon dioxide using continuous-flow isotope-ratio mass spectrometry. *Rapid Communications in Mass Spectrometry* 20(2):200–8.

Forster P, Ramaswamy V, Artaxo P, Berntsen T, Betts R, Fahey DW, Haywood J, Lean J, Lowe DC, Myhre G, Nganga J, Prinn R, Raga G, Schulz M, Van Dorland R. 2007. Changes in atmospheric constituents and in radiative forcing. In: Solomon S, Qin D, Manning M, Chen Z, Marquis M, Averyt KB, Tignor M, Miller HL, editors. *Climate Change 2007: The Physical Science Basis. Contribution of Working Group I to the Fourth Assessment Report of the Intergovernmental Panel on Climate Change*. Cambridge: Cambridge University Press. p 130–234.

Foulger BE, Simmonds PG. 1993. Ambient temperature gas purifier suitable for the trace analysis of carbon monoxide and hydrogen and the preparation of low-level carbon monoxide calibration standards in the field. *Journal of Chromatography* 630(1–2):257–63.

Grabowski KS, Knies DL, Tumey SJ, Pohlman JW, Mitchell CS, Coffin RB. 2004. Carbon pool analysis of methane hydrate regions in the seafloor by accelerator mass spectrometry. *Nuclear Instruments and Methods in Physics Research B* 223–224:435–40.

Haan D, Raynaud D. 1998. Ice core record of CO variations during the last two millennia: atmospheric implications and chemical interactions within the Greenland ice. *Tellus B* 50(3):253–62.

Hua Q, Jacobsen GE, Zoppi U, Lawson EM, Williams AA, Smith AM, McGann MJ. 2001. Progress in radiocarbon target preparation at the ANTARES AMS Centre. *Radiocarbon* 43(2A):275–82.

Hua Q, Zoppi U, Williams AA, Smith AM. 2004. Small-mass AMS radiocarbon analysis at ANTARES. *Nuclear Instruments and Methods in Physics Research B* 223–224:284–92.

Kennett JP, Cannariato KG, Hendy IL, Behl RJ. 2000. Carbon isotopic evidence for methane hydrate instability during Quaternary interstadials. *Science* 288(5463):128–33.

Kennett JP, Cannariato KG, Hendy IL, Behl RJ. 2003. *Methane Hydrates in Quaternary Climate Change: The Clathrate Gun Hypothesis*. Washington, DC: American Geophysical Union. 216 p.

Kessler JD, Reeburgh WS. 2005. Preparation of natural methane samples for stable isotope and radiocarbon analysis. *Limnology and Oceanography-Methods* 3: 408–18.

Kessler JD, Reeburgh WS, Southon J, Seifert R, Michaelis W, Tyler SC. 2006. Basin-wide estimates of the input of methane from seeps and clathrates to the Black Sea. *Earth and Planetary Science Letters* 243(3–4): 366–75.

Lal D, Jull AJT, Burr GS, Donahue DJ. 2000. On the characteristics of cosmogenic in situ ^{14}C in some GISP2 Holocene and late glacial ice samples. *Nuclear Instruments and Methods in Physics Research B* 172(1–4):623–31.

Lassey KR, Lowe DC, Smith AM. 2007. The atmospheric cycling of radiomethane and the "fossil fraction" of the methane source. *Atmospheric Chemistry and Physics* 7(8):2141–9.

Lowe DC, Brenninkmeijer CAM, Tyler SC, Dlugkencky EJ. 1991. Determination of the isotopic composition of atmospheric methane and its application in the Antarctic. *Journal of Geophysical Research* 96(D8): 15,455–67.

Milkov AV. 2004. Global estimates of hydrate-bound gas in marine sediments: how much is really out there? *Earth-Science Reviews* 66(3–4):183–97.

Mühle J, Lueker TJ, Su Y, Miller BR, Prather KA, Weiss RF. 2007. Trace gas and particulate emissions from

the 2003 southern California wildfires. *Journal of Geophysical Research* 112(D3): D03307, doi: 10.1029/2006JD007350.

Petrenko VV, Severinghaus JP, Brook EJ, Reeh N, Schaefer H. 2006. Gas records from the West Greenland ice margin covering the Last Glacial Termination: a horizontal ice core. *Quaternary Science Reviews* 25(9–10):865–75.

Petrenko VV, Severinghaus JP, Brook EJ, Mühle J, Headly M, Harth C, Schaefer H, Reeh N, Weiss RF, Lowe D, Smith AM. 2008. Instruments and Methods: A novel method for obtaining very large ancient air samples from ablating glacial ice for analyses of methane radiocarbon. *Journal of Glaciology* 54(185), in press.

Price PB. 2007. Microbial life in glacial ice and implications for a cold origin of life. *FEMS Microbiology Ecology* 59(2):217–31.

Pupek M, Assonov SS, Mühle J, Rhee TS, Oram D, Koeppel C, Slemr F, Brenninkmeijer CAM. 2005. Isotope analysis of hydrocarbons: trapping, recovering and archiving hydrocarbons and halocarbons separated from ambient air. *Rapid Communications in Mass Spectrometry* 19(4):455–60.

Quay P, Stutsman J, Wilbur D, Snover A, Dlugokencky E, Brown T. 1999. The isotopic composition of atmospheric methane. *Global Biogeochemical Cycles* 13(2):445–61.

Reeh N, Oerter H, Letréguilly A, Miller H, Hubberten H-W. 1991. A new, detailed Ice-Age oxygen-18 record from the ice-sheet margin in central West Greenland. *Global and Planetary Change* 4(4):373–83.

Schaefer H, Whiticar MJ, Brook EJ, Petrenko VV, Ferretti DF, Severinghaus JP. 2006. Ice record of $\delta^{13}C$ for atmospheric CH_4 across the Younger Dryas-Preboreal transition. *Science* 313(5790):1109–12.

Smith AM, Levchenko VA, Etheridge DM, Lowe DC, Hua Q, Trudinger CM, Zoppi U, Elcheikh A. 2000. In search of in-situ radiocarbon in Law Dome ice and firn. *Nuclear Instruments and Methods in Physics Research B* 172(1–4):610–22.

Smith AM, Petrenko VV, Hua Q, Southon J, Brailsford G. 2007. The effect of N_2O, catalyst, and means of water vapor removal on the graphitization of small CO_2 samples. *Radiocarbon* 49(2):245–54.

Sowers T. 2006. Late Quaternary atmospheric CH_4 isotope record suggests marine clathrates are stable. *Science* 311(5762):838–40.

Stuiver M. 1983. International agreements and the use of the new oxalic acid standard. *Radiocarbon* 25(2):793–5.

Stuiver M, Polach HA. 1977. Discussion: reporting of ^{14}C data. *Radiocarbon* 19(3):355–63.

Van de Wal RSW, Meijer HAJ, de Rooij M, van der Veen C. 2007. Radiocarbon analyses along the EDML ice core in Antarctica. *Tellus B* 59(1):157–65.

Wahlen M, Tanaka N, Henry R, Deck B, Zeglen J, Vogel JS, Southon J, Shemesh A, Fairbanks R, Broecker W. 1989. Carbon-14 in methane sources and in atmospheric methane: the contribution from fossil carbon. *Science* 245(4915):286–90.

Winckler G, Aeschbach-Hertig W, Holocher J, Kipfer R, Levin I, Poss C, Rehder G, Suess E, Schlosser P. 2002. Noble gases and radiocarbon in natural gas hydrates. *Geophysical Research Letters* 29(10): doi: 10.1029/2001GL014013.